



## Charge Transfer and Optical Characteristics of cyclopenta-diene based Oligomers

Mrs. Jothi Balakrishnan<sup>1</sup>, Mr. Stephen A. David<sup>2</sup>, Mr. Palanisamy Subramaniam<sup>3</sup>,  
Mr. Selvaraju Karuppanan<sup>4</sup>

<sup>1</sup> Department of Physics, KandaswamiKandar 'sCollege, Velur 638182 Tamilnadu, India

<sup>2</sup> Department of Physics, PSG college of Arts and Science, Coimbatore 641014 Tamilnadu, India

<sup>3,4</sup> Department of Physics, Kandaswami Kandar 's College, Velur 638182 Tamilnadu, India

**ABSTRACT:** 1,4-bis(2-(cyclopenta-1,3-dien-1-yl)ethyl)cyclopenta-1,3-diene [CCD] is one of the interesting oligomer with high charge carrier mobility and chemical stability. Based on the density functional theory (DFT), the electronic characteristics of four CCD molecules with various hetero atom substituents are investigated. The electronic of four CCD molecules with different hetero atom substituents are explored based on the density functional theory (DFT). The effects of substituents on the molecular structure, molecular orbitals, ionization energies, electron affinities, reorganization energy and crystal packing are analysed in detail to clarify the structure-property relationship of the studied molecules. The different crystal packing arrangements and intermolecular interactions of the studied molecules lead to differences in transfer integrals when introducing different substituents to the CCD molecule.

**KEYWORDS:** DFT Theory, Ionization energies, Molecular orbitals, Reorganization energy

### 1. INTRODUCTION

In comparison to inorganic semiconductors, organic semiconductors have a number of advantages, including flexibility, transparency, affordability, ease of large-area processing, and phenomenal structural modification space (Oh J Y, *et al*, 2016)–(Chen Z, *et al*, 2012). They now serve as the fundamental building blocks of modern organic photoelectronic and microelectronic devices. Organic photovoltaics (OPV), organic light-emitting displays (OLED), organic field effect transistors (OFETs), and organic sensors (Zhang X, *et al*, 2018)– (Zhang Y, *et al*, (2008) are just a few of the many potential applications for them. The development of n-type organic semiconductors is limited, while the majority of investigated organic semiconductors are p-type. The majority of organic semiconductors have access points of Donor-Acceptor, Acceptor-Acceptor, or Donor-Acceptor-Acceptor and comprise electron-rich donors and electron deficient acceptors. Common donors include benzene (Kitamura M, *et al*, 2008), acene, thiophene, and thieno[3,2b]thiophene (Sirringhaus H, *et al*, 1999),. Because of their significant p-conjugation and remarkable chemical and physical properties, oligothiophenes, linear arenes, and their derivatives are the most extensively investigated organic semiconductors among all organic p-type and n-type conjugated materials. Pentacene, (Bhatia R, *et al*, 2019), a common linear arene and the current industry standard for field-effect mobility in thin film devices, has a hole mobility of up to 5.5 cm<sup>2</sup>/Vs. It appeared that the fused thiophenes and cyclopentadienes (Levandowski B J, *et al*, 2021), were well known for their higher stability. Moreover, thiophene-based materials show a range of intra- and intermolecular interactions, including pi-pi stacking, weak hydrogen bonds, and van der Waals interactions (Pham P T T, *et al*, 2014),. Particularly, the high polarizability of the sulphur atom in thiophene rings causes sulfur-sulfur interactions, which are crucial for achieving high charge mobility and establishing the transport network (Duan Y A, *et al*, 2014), These interactions may have a significant impact on the solid-state packing of the species involved. Thus cyclopenta-dienes based molecules were incorporated into the new design approach for OSCs in order to produce high-performance OFETs.

The optoelectronic properties of these compounds appear to be significantly influenced by the substituted position of the hetero atoms; Nitrogen, Oxygen and Sulphur in the 5-membered ring, according to earlier studies (Zhang Y, *et al*, 2008), (Paramasivam M, *et al*, 2018), – (Liu J, *et al*, 2013). To discover appropriate materials for device applications, however, design and comprehension of the impact of various substitution on optoelectronic properties are required. Electronic structure simulations have been carried out in the present work to undertake theoretical investigations on the structural, optoelectronic, and charge transport



features of newly developed 1,4-bis(2-(cyclopenta-1,3-dien-1-yl)ethyl)cyclopenta-1,3-diene [CCD] and their derivatives. Figure 1 shows the chemical structure of the studied molecules.

## 2. COMPUTATIONAL METHODOLOGY

The neutral and ionic state geometries of CCD and its derivatives have been optimised using the density functional theory (DFT) method with the B3LYP (Lee C, et al, 1988) – (Hohenberg P, et al, 1964) functional and 631G+(d,p) basis set (Del Bene J E, et al, 1995). According to previous DFT research (Chen H Y, et al, 2006), the results obtained using the B3LYP functional are recognised for their accurate predictions of the structural properties and agree with experimental data. The ideal geometry of the molecules under study was confirmed by vibrational frequency analysis with zero imaginary frequencies. The UV-vis absorption spectra of all the studied molecules under investigation have been calculated using TD-DFT (Furche F, et al, 2005) calculations at the CAM-B3LYP/6-311g(d,p) level of theory (Yanai T, et al, 2004). The long-range corrected functional CAM-B3LYP yields precise results for calculations of excited states. The calculations above were performed using the Gaussian09 software suite (Frisch G M J, et al., 2009).

The examined molecule's ionisation potential (IP), electron affinity (EA), hole extraction potential (HEP), and electron extraction potential (EEP) were calculated using the following equations (Tavernier H L, et al, 1998), (Krishnan S, et al, 2021).

$$VIP = E^+(g^0) - E^0(g^0) \quad (1)$$

$$AIP = E^+(g^+) - E^0(g^0) \quad (2)$$

$$VEA = E^0(g^0) - E^-(g^0) \quad (3)$$

$$AEA = E^0(g^0) - E^-(g^-) \quad (4)$$

$$HEP = E^+(g^+) - E^0(g^+) \quad (5)$$

$$EEP = E^0(g^-) - E^-(g^-) \quad (6)$$

Thus,  $E_0(g_0)$  denotes the optimal ground state energy of the neutral molecule,  $E_{\pm}(g_0)$  denotes the total energy of an ion in optimised neutral geometry,  $E_{\pm}(g_{\pm})$  denotes the energy of an ion in optimised ionic geometry, and  $E_0(g_{\pm})$  denotes the energy of the neutral molecule in ionic geometry.

The external contribution to the reorganisation energy is not included in the computation of the internal reorganisation energy in the present work, which uses the adiabatic potential energy surface approach. The energy change caused by structural relaxation while shifting from an electro-neutral to a charged molecular state, and vice versa, is provided by Equations.

$$\lambda_{\pm} = (E^{\pm}(g^0) - E^{\pm}(g^{\pm})) + (E^0(g^{\pm}) - E^0(g^0)) \quad (7)$$

Using the CrystalExplorer17 software (Spackman P R, et al, 2021), the Hirshfeld surface and 2D fingerprint were plotted in the investigation of the interactions between the molecules in the crystal structure.

## 3. RESULTS AND DISCUSSION

### 3.1 Molecular structure and frontier molecular orbitals.

The geometry of CCD and their derivative compounds that were optimized at the B3LYP/6-31G+(d,p) level of theory is shown in Figure 2. One of the key factors that controls the charge carrier mobility in conjugated organic compounds is planarity. The optimal geometry of the investigated compounds reveals that the all the three cyclopentane with different hetero atom substitutions are exhibited the co-planarity with the maximum deviation of about 2 Å from the plane of the rings in CCD-S molecule.

The molecules' optoelectronic and charge transport capabilities depend on the energy and alignment of their frontier molecular orbitals (FMO) (Khan M U, et al, 2018) – (Khan M U, et al, 2019). Thus, while adjusting the optical and electrical properties of the molecules, a thorough investigation of the FMO of organic molecules is crucial. In Figure 3, the examined compounds' LUMO and HOMO density plots are displayed. Figure 3 illustrates that, the substitution of the hetero atoms in the cyclopentane ring does not affect the HOMO and LUMO of CCD molecules. HOMO is primarily focused on double bonds, i.e., on the components C, O, and N. The LUMO, on the other hand, is primarily focused on single bonds, i.e., on S, C, H, and other components.



The HOMOLUMO energy gap of organic semiconductors typically lies between 1.4 and 4.2 eV on average (Chen Z, et al, 2017). The energy gap of the molecules under study extends from 2.35 to 2.95 eV, according to Figure 4 and thus all of the investigated compounds are therefore organic semiconductors. According to Figure 3, the energy gap (Eg) widens as heteroatoms are substituted on the cyclopentane rings of the CCD molecule. The CCD molecule with an NH substitution has the maximum band gap of 2.95 eV. The predicted absorption energy for the electronic transition from HOMO to LUMO has been shown to be comparable to the energy gap (Eg) value. The molecules with the smallest energy gap (Eg) have the smallest absorption energy or the longest wavelength of absorption, as would be predicted.

### 3.2 Absorption spectra

The absorption spectrum is a crucial factor in determining the feasibility of the compounds under study in the optoelectronic applications. Figure 5 illustrates the absorption spectra of the CCD-based molecules computed using the TD-DFT approach at the B3LYP/6-31+g(d,p) level of theory. To better understand the characteristics and energies of singlet-singlet electronic transitions, the first 10 low-lying electronic transition energies have been computed. Table 1 provides a summary of the calculated absorption wavelength, energy, oscillator strength, and associated electronic transitions. The absorption transitions with oscillator strengths greater than 0.01 are taken into account for the further discussion. The excitation of an electron from HOMO to LUMO causes the lowest energy transition for all the molecules under study.

The CCD molecule's highest absorption peak is visible at 530 nm, and this wavelength correlate to the electronic transitions from HOMO to LUMO. As seen in Figure 4, the substitution of hetero atoms had a major impact on the absorption spectrum as revealed from the changes in the absorption maximum ( $\lambda_{max}$ ) of CCD-S, CCD-NH and CCD-O molecules. From Figure 4, it can be seen that the substitution of hetero atom on the CCD molecule increased the peak's strength. The maximum absorption wavelength of the hetero atom substituted CCD molecules exhibits blueshift in comparison to the CCD molecule. The maximum blueshift in the  $\lambda_{max}$  has been observed to be 94 nm greater for NH substituted CCD molecule.

**Table 1:** Calculated Absorption Energies (in eV), Wavelengths (in nm), Oscillator Strengths (in au), and the corresponding orbital transitions of studied CCD molecules calculated at the B3LYP/6-31G+(d,p) Level of Theory

Molecules	Absorption energy (eV)	Absorption wavelength (nm)	Oscillator strength	Orbital transitions
CCD	2.26	530	1.36	HOMO->LUMO (102%)
	2.77	433	0.03	H-1->LUMO (42%), HOMO->L+1 (56%)
	3.44	349	0.14	H-1->LUMO (49%), HOMO->L+1 (37%), HOMO->L+2 (11%)
	3.54	339	0.03	H-2->LUMO (13%), HOMO->L+2 (73%)
	4.17	288	0.05	H-2->LUMO (40%), H-1->L+1 (48%)
CCD-S	2.58	465	1.49	HOMO->LUMO (101%)
	3.19	376	0.04	H-1->LUMO (42%), HOMO->L+1 (56%)
	3.73	321	0.09	H-1->LUMO (56%), HOMO->L+1 (40%)
	4.19	286	0.09	H-4->LUMO (41%), H-3->LUMO (26%), H-2->LUMO (26%)
	4.30	279	0.08	H-5->LUMO (19%), H-1->L+1 (77%)
CCD-NH	2.75	436	1.47	HOMO->LUMO (100%)



	3.37	356	0.08	H-1->LUMO (34%), HOMO->L+1 (64%)
	3.91	307	0.22	H-1->LUMO (64%), HOMO->L+1 (33%)
	4.42	271	0.07	H-2->LUMO (34%), H-1->L+1 (64%)
CCD-O	2.72	440	1.38	HOMO->LUMO (101%)
	3.31	363	0.04	H-1->LUMO (41%), HOMO->L+1 (57%)
	3.97	303	0.38	H-1->LUMO (57%), HOMO->L+1 (41%)
	4.39	273	0.03	H-2->LUMO (64%), H-1->L+1 (26%)
	4.49	267	0.05	H-1->L+1 (61%), HOMO->L+5 (28%)

### 3.3 Ionic State Properties

In semiconductor materials, such as field-effect organic transistors or organic light-emitting diodes, ionisation potential (IP) and electron affinity (EA), which reflect the injection capabilities of holes and electrons and are connected to the redox energy of electronic devices and environmental stability, are significant parameters. In general, p-type semiconductors need a low IP while n-type semiconductors need a high EA. It is typical to have both low IP and high EA for ambipolar semiconductor materials. According to previous research studies, molecular materials can generally exhibit stable n-type semiconductor characteristics in the air when their EA is in the range from 1 to 3 eV (Liu C C, et al, 2010), which can efficiently overcome the electron injection barrier and assure effective injection into LUMO. The vertical ionization potential (IPV), adiabatic ionization potential (IPA), vertical electron affinity (EAV), adiabatic electron affinity (EAA), HEP and EEP of cyclopentadithiophene derivatives calculated using Eq. (1)– (6) are summarized in Table 2.

When various hetero atoms were added to the cyclopentane rings, the vertical IPs of the CCD molecule, which have IP<sub>v</sub> and IP<sub>a</sub> of 5.87 and 5.71 eV respectively, undergone a small variation. Among the studied compounds, CCD-S with the sulphur substitution has the greatest IPs [6.36/6.22 eV]. All of these molecules are more stable and have antioxidative qualities in their natural environments, as shown by the fact that their vertical IPs are higher than those of pentacene (5.94 eV) (Wang L, et al, 2016), and the stable p-type material sexthiophene (5.80 eV) (Huang J D, et al, 2011). In comparison to CCD and CCD-S molecules, the IPs of CCD-NH and CCD-O molecules decreased with the adiabatic and vertical ionisation potentials of 5.84/5.69 eV and 6.27/6.13 eV, respectively. Thus, the hole injection from the metallic electrodes is facilitated. CCD and CCD-S molecules have a lower lying LUMO level than the other CCD based compounds, as seen in Figure 4, which enhances their ability to accept electrons. Injecting an electron into the cationic geometry of the aNDT2 molecule is easier than that of the other analysed molecules because the HEP of the CCD-NH molecule (5.53 eV) is determined to be lower than that of other assessed molecules. Moreover, both the CCDNH and CCD-O have reduced EEPs. The trend in the difference between IP and EA is consistent with the calculated FMO energy gap (E<sub>g</sub>).

**Table 2:** The calculated vertical ionization potential (VIP), adiabatic ionization potential (AIP), vertical electron affinities (VEA), adiabatic electron affinities (AEA), electron extraction potential (EEP), hole extraction potential (HEP), hole reorganization energy ( $\lambda_+$ ), and electron reorganization energy ( $\lambda_-$ ) of the studied CCD based molecules in eV

Molecules	VIP	AIP	VEA	AEA	HEP	EEP	$\lambda_-$	$\lambda_+$
CCD	5.87	5.71	1.07	1.22	5.55	1.36	0.29	0.32
CCD-S	6.36	6.22	1.14	1.27	6.07	1.40	0.27	0.30
CCD-NH	5.84	5.69	0.35	0.47	5.53	0.61	0.26	0.31
CCD-O	6.27	6.13	0.79	0.92	5.99	1.06	0.27	0.28



### 3.4 Reorganization energies

One of the key elements affecting the rate of charge transport in organic semiconductors is the reorganisation energy. The lower reorganisation energy allows for the higher charge transfer rate. Using Eq. (7) at the B3LYP/631G+(d,p) level of theory, the reorganisation energy ( $\lambda_{+/-}$ ) of CCD derivatives in the presence of excess positive and negative charges has been determined and is presented in Table 2. In the presence of positive and negative charges, CCD has a maximum reorganisation energy of 0.29 eV and 0.32 eV respectively among the molecules under study. According to Table 2, the reorganisation energy ( $\lambda_{\cdot}$ ) for the other CCD derivatives is around 0.27 eV in the presence of negative charge. Internal rearrangement energies for electrons and holes in CCD-O are 0.27 eV and 0.28 eV, respectively and thus it reveals that energy associated with structural relaxation during hole and electron transport, is in agreement with results from the structural parameters of neutral, cationic, and anionic geometries.

### 3.5 Crystal structures of CCD derivatives

The Polymorph Predictor module of the Materials Studio package (17.1.0.48) (2019), has predicted the crystal structures of the CCD-systems using their ideal gas-phase conformations. For this calculation, the Polymorph Predictor quality was set to the default fine level, which anneals the sample with a heating factor of 0.025 between 300.0 K and 100000.0 K using the Monte Carlo simulation algorithm (Howell S C, et al, 2016). This algorithm have the maximum of 7000 steps, and it can tolerate 12 consecutive steps before cooling. We've integrated the Dreiding forcefield and Gasteiger charges in this case. In the Cambridge Structural Database, the ten most common space groups for organic compounds are listed as P21/c, P1, P212121, C2/c, P21, Pbcn, Pna21, and Pbcn. We restrict our prediction to these ten space groups. The crystal structures were ranked by total energy, with the lowest structure being utilised as the basis for subsequent calculations. Table 3 provides a summary of the CCD and its derivative's crystal parameters with hetero atom substitutions.

**Table 3:** The unit cell parameters of predicted crystal structures of CCD based molecule.

Structure	Space group	a(Å)	b(Å)	c(Å)	$\alpha(^{\circ})$	$\beta(^{\circ})$	$\gamma(^{\circ})$	Volume (Å <sup>3</sup> )
CCD	P212121	31.325	11.770	4.037	90.0	90.0	90.0	1488.28
CCD-S	P212121	33.109	3.916	11.637	90.0	90.0	90.0	1508.68
CCD-NH	C2	11.394	3.653	33.021	90.0	88.9	90.0	1374.16
CCD-O	Pbcn	32.816	7.155	11.394	90.0	90.0	90.0	2675.27

### 3.6 Hirshfeld surface analysis

The Hirshfeld surface analysis aids in quantifying and visualising intermolecular interactions through the use of various colours and intensities in graphical depiction. Hirshfeld surface analysis has been used to study numerous intermolecular interactions in the crystal structure of organic molecules and complexes (Van Thong P, *et al*, 2022), AlResayes S I, *et al*, 2020). The normalised contact distance ( $d_{norm}$ ) maps of CCD and their functionalized molecules are displayed in Figure 6. Blue surfaces, indicates the interactions that are farther apart, red surfaces display connections that are closer together than the Van der Waals radii (distance contact). The distance denoted by the white surfaces is represented by the sum of the van der Waals radii. Figure 6 also displays the 2D fingerprint plots and fragment patches, of CCD systems. The  $d_e$  and  $d_i$  on the plots represent the exterior and interior distances from the surface to the nearest atom centre. Without a contribution, plot points are grey, whereas those that do range from blue to green to red for the largest contributions. The H...H interaction significantly affects the overall surface in all CCD systems. In addition to H...H interactions, N...H/H...N and O...H/H...O were the second-largest contributions in CCD-NH and CCD-O molecule.

## 4. CONCLUSION

Investigations on the electronic and optical properties of 1,4-bis(2-(cyclopenta-1,3-dien-1-yl)ethyl)cyclopenta-1,3-diene [CCD] based molecules with various heteroatom substitutions. Sulfur, Nitrogen, and Oxygen heteroatoms were substituted into each of the three cyclopentane rings, forming the molecules CCD-S, CCD-NH, and CCD-O, respectively. When these substitutions were





made, it changed the molecule's energy levels, which significantly changed the absorption spectra as compared to the unsubstituted CCD molecule. It was found that the CCD molecules have promise in optoelectronics by the analysis of their absorption spectra. The unsubstituted CCD and CCD-S molecules are n-type semiconducting materials, according to the predicted ionisation characteristics, while the CCD-NH and CCD-O molecules are p-type materials. The current work sheds information on the development of novel organic semiconductors for optoelectronic uses. Among the molecules, CCD has a maximum reorganisation energy of 0.29 eV and 0.32 eV, in the presence of positive and negative charges. In order to understand the intermolecular interactions between CCD molecules. From the electronic investigation of CCD systems, it was concluded that, CCD and CCD-S exhibits n type characteristics, while CCD-NH and CCD-O reveals its p-type characteristics. Hirshfeld surface analysis was also performed. The 2D fingerprint plot of the crystal structures of the CCD systems was examined, and it was found that the O...H/H...O, S...H/H...S, and N...H/H...N interactions were the most prominent considerations after the H...H interactions. This work thus highlights novel organic semiconductors for optoelectronic applications.

## REFERENCES

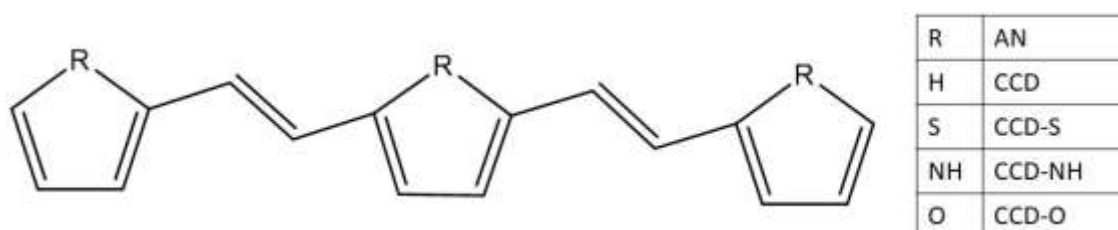
1. Oh J Y, *et al*, (2016), Intrinsically stretchable and healable semiconducting polymer for organic transistors, 539,(7629), 411–415, doi: 10.1038/nature20102.
2. Zhang J, *et al*, (2018), Material insights and challenges for non-fullerene organic solar cells based on small molecular acceptors, *Nat Energy*, 3, (9), 720–731, doi: 10.1038/s41560-018-0181-5.
3. Freudenberg J, *et al*, (2018), Immobilization Strategies for Organic Semiconducting Conjugated Polymers, *Chem Rev*, 118, (11), 5598–5689, doi: 10.1021/acs.chemrev.8b00063.
4. Chen Z, *et al*, (2012), High-Performance Ambipolar Diketopyrrolopyrrole-Thieno[3,2-b]thiophene Copolymer Field-Effect Transistors with Balanced Hole and Electron Mobilities, *Advanced Materials*, 24, (5), 647–652, <https://doi.org/10.1002/adma.201102786>.
5. Zhang X, *et al*, (2018), Organic Semiconductor Single Crystals for Electronics and Photonics,” *Advanced Materials*. doi:10.1002/adma.201801048.
6. Kotadiya N B, *et al.*, (2018), Universal strategy for Ohmic hole injection into organic semiconductors with high ionization energies, *Nat Mater*, 17, (4), 329–334, doi: 10.1038/s41563-018-0022-8.
7. Zhang Y, *et al*, (2008), Heteroatom Substitution of Oligothiophenes: From Good p-Type Semiconductors to Good Ambipolar Semiconductors for Organic Field-Effect Transistors, *The Journal of Physical Chemistry* 112, (13), 5148–5159, doi: 10.1021/jp710123r.
8. Kitamura M, *et al*, (2008), Pentacene-based organic field-effect transistors, *Journal of Physics: Condensed Matter*, 20, (18), 184011, doi: 10.1088/0953-8984/20/18/184011.
9. Siringhaus H, *et al*, (1999), Two-dimensional charge transport in self-organized, high-mobility conjugated polymers, doi: 10.1038/44359.
10. Bhatia R, *et al*, (2019), Methodologies for the synthesis of pentacene and its derivatives, *Journal of Saudi Chemical Society*, 23, (7), 925–937, <https://doi.org/10.1016/j.jscs.2019.04.001>.
11. Levandowski B J, *et al*, (2021), Click Chemistry with Cyclopentadiene, 121, (12), 6777–6801, doi: 10.1021/acs.chemrev.0c01055.
12. Pham P T T, *et al*, (2014), Inter- and Intramolecular Interactions in Some Bromo- and Tricyanovinyl-Substituted Thiophenes and Ethylenedioxythiophenes, *Cryst Growth Des*, 14, (3), 916–922, Mar. 2014, doi: 10.1021/cg401513n.
13. Duan Y A, *et al*, (2014), Theoretical studies on the hole transport property of tetrathienoarene derivatives: The influence of the position of sulfur atom, substituent and  $\pi$ -conjugated core, *Org Electron*, 15, (2), 602–613, <https://doi.org/10.1016/j.orgel.2013.12.011>.
14. Paramasivam M, *et al*, (2018), The impact of heteroatom substitution on cross-conjugation and its effect on the photovoltaic performance of DSSCs – a computational investigation of linear vs. cross-conjugated anchoring units, *Physical Chemistry Chemical Physics*, 20, (35), 22660–22673, doi: 10.1039/C8CP02709A.
15. Hu Z, *et al*, (2016), Effects of heteroatom substitution in spiro-bifluorene hole transport materials, *Chem Sci*, 7, (8), 5007–5012, 2016, doi: 10.1039/C6SC00973E.



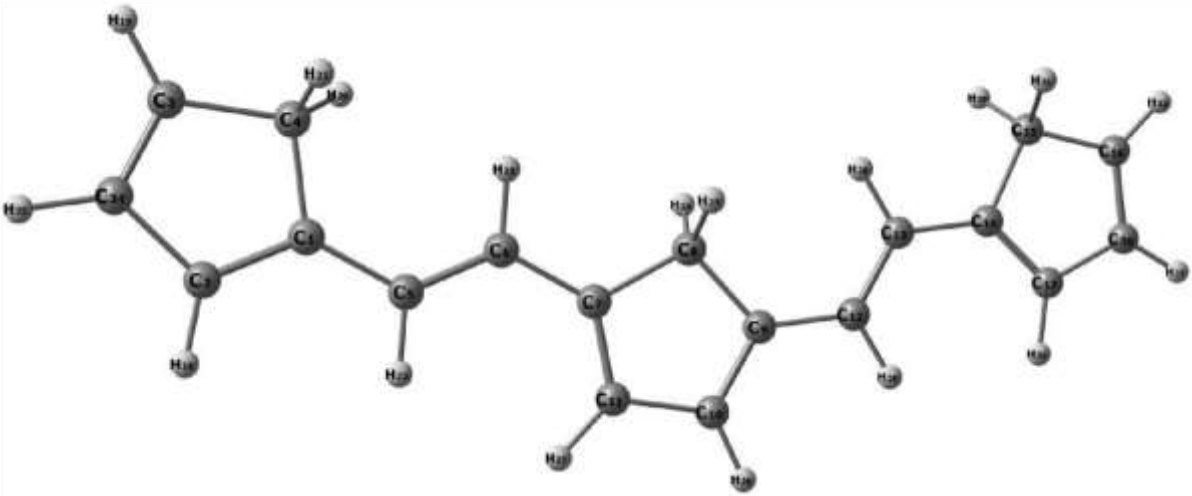
16. Liu J, et al, (2013), Effects of Heteroatom Substitutions on the Crystal Structure, Film Formation, and Optoelectronic Properties of Diketopyrrolopyrrole-Based Materials, *Adv Funct Mater*, 23, (1), 47–56, <https://doi.org/10.1002/adfm.201201599>.
17. Lee C, et al, (1988), Development of the Colle-Salvetti correlation-energy formula into a functional of the electron density, *Phys Rev B*, 37, (2), 785–789, doi: 10.1103/physrevb.37.785.
18. Becke A D, (1992), Density-functional thermochemistry. I. The effect of the exchange-only gradient correction, *Journal of Chemical Physics*, doi: 10.1063/1.462066.
19. Becke A D, (1988), Density-functional exchange-energy approximation with correct asymptotic behavior, *Phys Rev A (Coll Park)*, doi: 10.1103/PhysRevA.38.3098.
20. Hohenberg P, et al, (1964), Inhomogeneous electron gas, *Physical Review*, doi: 10.1103/PhysRev.136.B864.
21. Del Bene J E, et al, (1995), Properties of Hydrogen-Bonded Complexes Obtained from the B3LYP Functional with 6-31G(d,p) and 6-31+G(d,p) Basis Sets: Comparison with MP2/6-31+G(d,p) Results and Experimental Data, *J Phys Chem*, 99, (27), 10705–10707, doi: 10.1021/j100027a005.
22. Chen H Y, et al, (2006), Toward the rational design of functionalized pentacenes: Reduction of the impact of functionalization on the reorganization energy, *ChemPhysChem*, doi: 10.1002/cphc.200600266.
23. Furche F, et al, (2005), Density Functional Methods for Excited States: Equilibrium Structure and Electronic Spectra, *Theoretical and Computational Chemistry*. Elsevier, 93–128, 2005. doi: 10.1016/s1380-7323(05)80020-2.
24. Yanai T, et al, (2004), A new hybrid exchange–correlation functional using the Coulomb-attenuating method (CAMB3LYP), *Chem Phys Lett*, 393, (1–3), 51–57, doi: 10.1016/J.CPLETT.2004.06.011.
25. Frisch G M J, et al., (2009), Gaussian 09, Revision E. 01; Gaussian, *Gaussian, Inc.: Wallingford, CT*.
26. Tavernier H L, et al, (1998), Solvent Reorganization Energy and Free Energy Change for Donor/Acceptor Electron Transfer at Micelle Surfaces: Theory and Experiment, *J Phys Chem B*, 102, (31), 6078–6088, doi: 10.1021/jp981754r.
27. Krishnan S, et al, (2021), The influence of the shape and configuration of sensitizer molecules on the efficiency of DSSCs: a theoretical insight, *RSC Adv*, 11, (10), 5556–5567, doi: 10.1039/D0RA10613E.
28. Spackman P R, et al, (2021), CrystalExplorer: A program for Hirshfeld surface analysis, visualization and quantitative analysis of molecular crystals, *J Appl Crystallogr*, doi: 10.1107/S1600576721002910.
29. Khan M U, et al, (2018), First Theoretical Framework of Triphenylamine–Dicyanovinylene-Based Nonlinear Optical Dyes: Structural Modification of  $\pi$ -Linkers, *The Journal of Physical Chemistry C*, 122, (7), 4009–4018, doi: 10.1021/acs.jpcc.7b12293.
30. Layaida H, et al, (2022), Synthesis, spectroscopic characterization, density functional theory study, antimicrobial and antioxidant activities of curcumin and alanine-curcumin Schiff base,” *J Biomol Struct Dyn*, . 1–16 doi: 10.1080/07391102.2022.2123043.
31. Janjua M R S A, et al, (2012), Effect of  $\pi$ -conjugation spacer (CC) on the first hyperpolarizabilities of polymeric chain containing polyoxometalate cluster as a side-chain pendant: A DFT study, *ComputTheor Chem*, 994, 34–40, <https://doi.org/10.1016/j.comptc.2012.06.011>.
32. Khan M U, et al, (2019) First theoretical probe for efficient enhancement of nonlinear optical properties of quinacridone based compounds through various modifications, *Chem Phys Lett*, 715, 222–230, <https://doi.org/10.1016/j.cplett.2018.11.051>.
33. Chen Z, et al, (2017), Density functional theory calculations of charge transport properties of ‘Plate-like’ coronene topological structures, *Journal of Chemical Sciences*, doi:10.1007/s12039-017-1351-x.
34. Liu C C, et al, (2010), Cyanated Pentaceno[2,3-c]chalcogenophenes for Potential Application in Air-Stable Ambipolar Organic Thin-Film Transistors, *The Journal of Physical Chemistry C*, 114, (50), 22316–22321, doi: 10.1021/jp1099464.
35. Wang L, et al, (2016), A theoretical study of the electronic structure and charge transport properties of thieno[2,3b]benzothiophene based derivatives, *Physical Chemistry Chemical Physics*, doi: 10.1039/c5cp07879b.
36. Huang J D, et al, (2011), Simulation of hole mobility in  $\alpha$ -oligofuran crystals, *Journal of Physical Chemistry B*, doi: 10.1021/jp108125q.

37. (2019), Overview of BIOVIA Materials Studio, LAMMPS, and GROMACS, *Molecular Dynamics Simulation of Nanocomposites Using BIOVIA Materials Studio, Lammmps and Gromacs*. Elsevier, 39–100, doi: 10.1016/b978-0-12816954-4.00002-4.
38. Howell S C, et al, (2016), Monte Carlo simulation algorithm for B-DNA, *J Comput Chem*, doi: 10.1002/jcc.24474.
39. Van Thong P, et al, (2022), NMR investigations on a series of diplatinum(II) complexes possessing phenylpropenoids in CDCl<sub>3</sub> and CD<sub>3</sub>CN: Crystal structure of a mononuclear platinum complex, *Polyhedron*, doi: 10.1016/j.poly.2021.115612.
40. Al-Resayes S I, et al, (2020), Structural and theoretical investigations, Hirshfeld surface analyses, and cytotoxicity of a naphthalene-based chiral compound, *ACS Omega*, doi: 10.1021/acsomega.0c03376.

### A. Figures



**Fig 1:** Chemical structures and their abbreviated notations (AN) of the studied CCD-based molecules

Molecule	Optimized geometry
CCD	



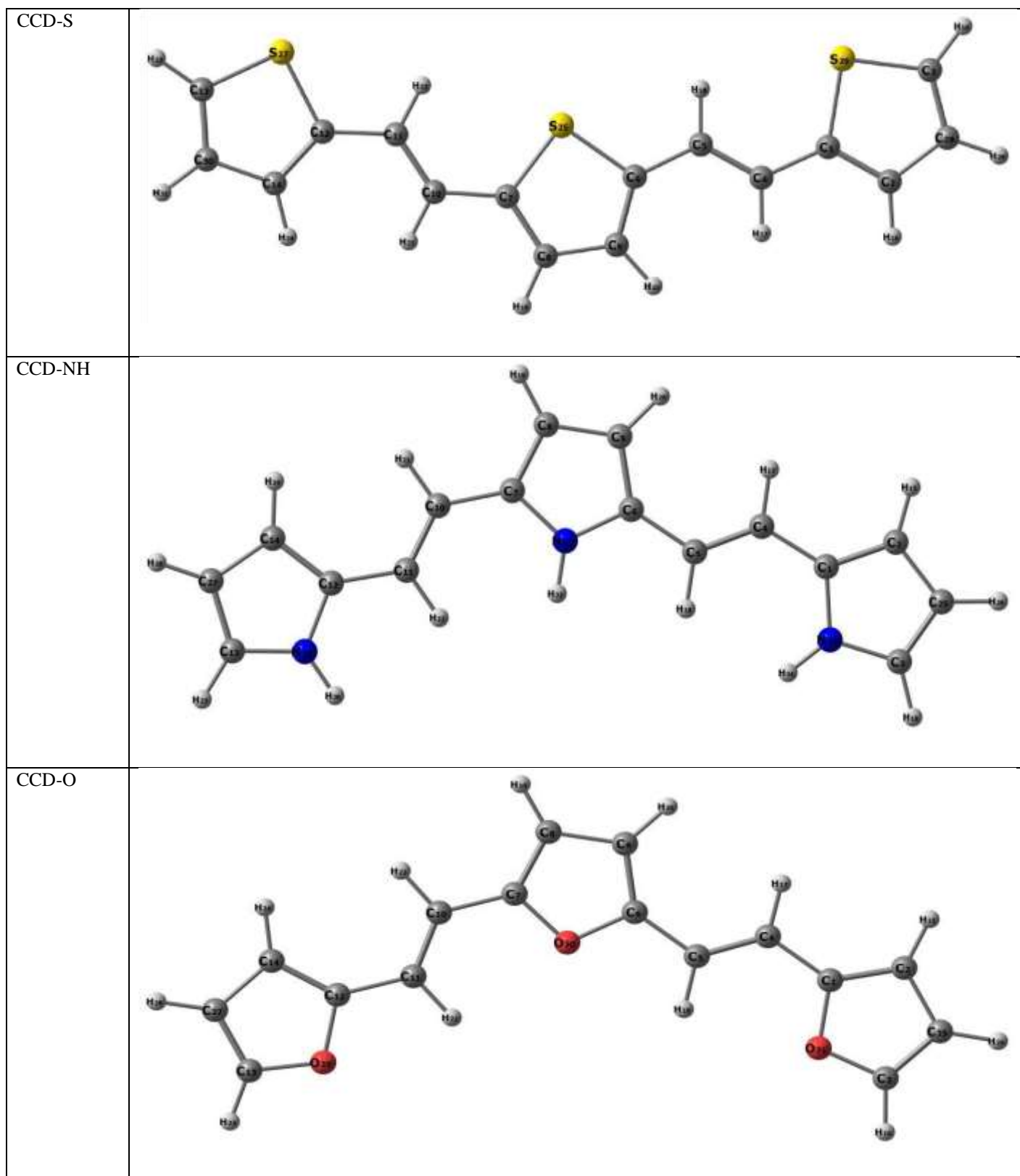


Fig 2: Optimized geometry of CCD and its derivatives at B3LYP/6-31+G(d,p) level of theory.

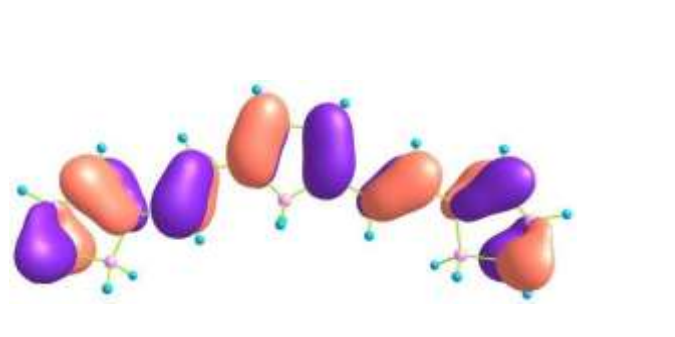
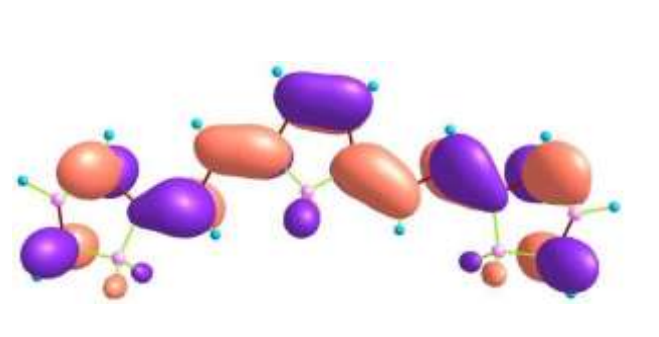
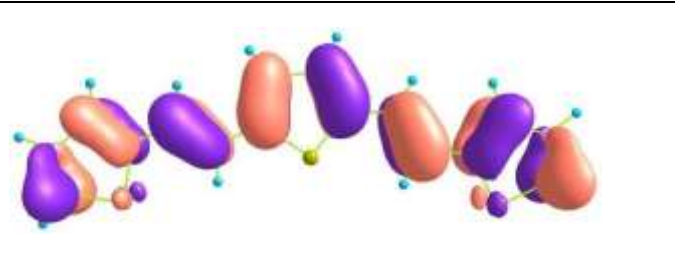
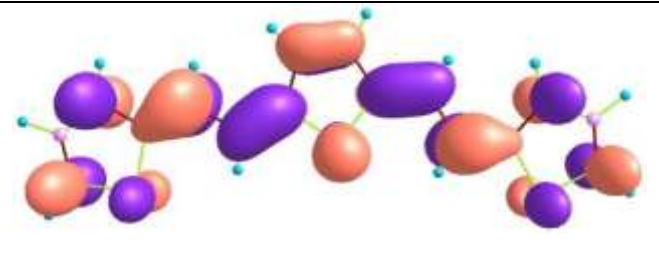
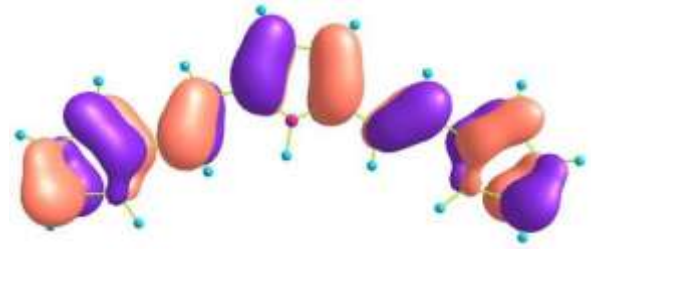
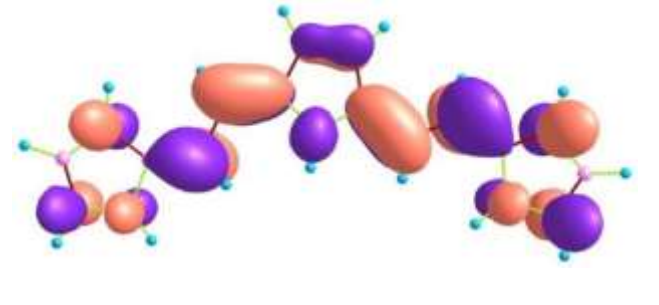
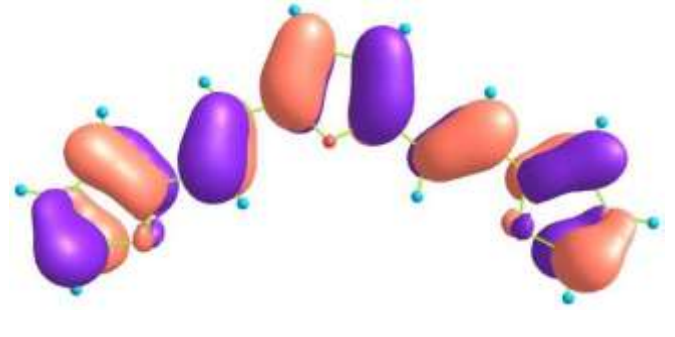
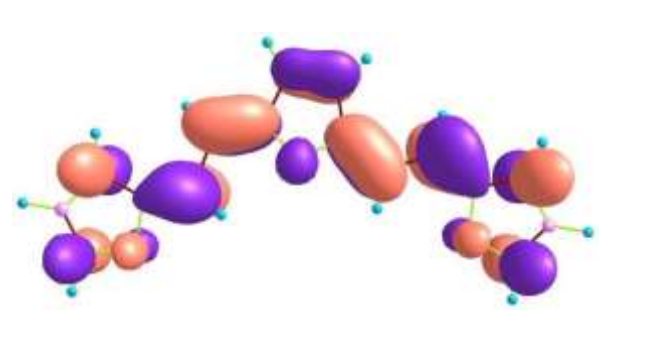
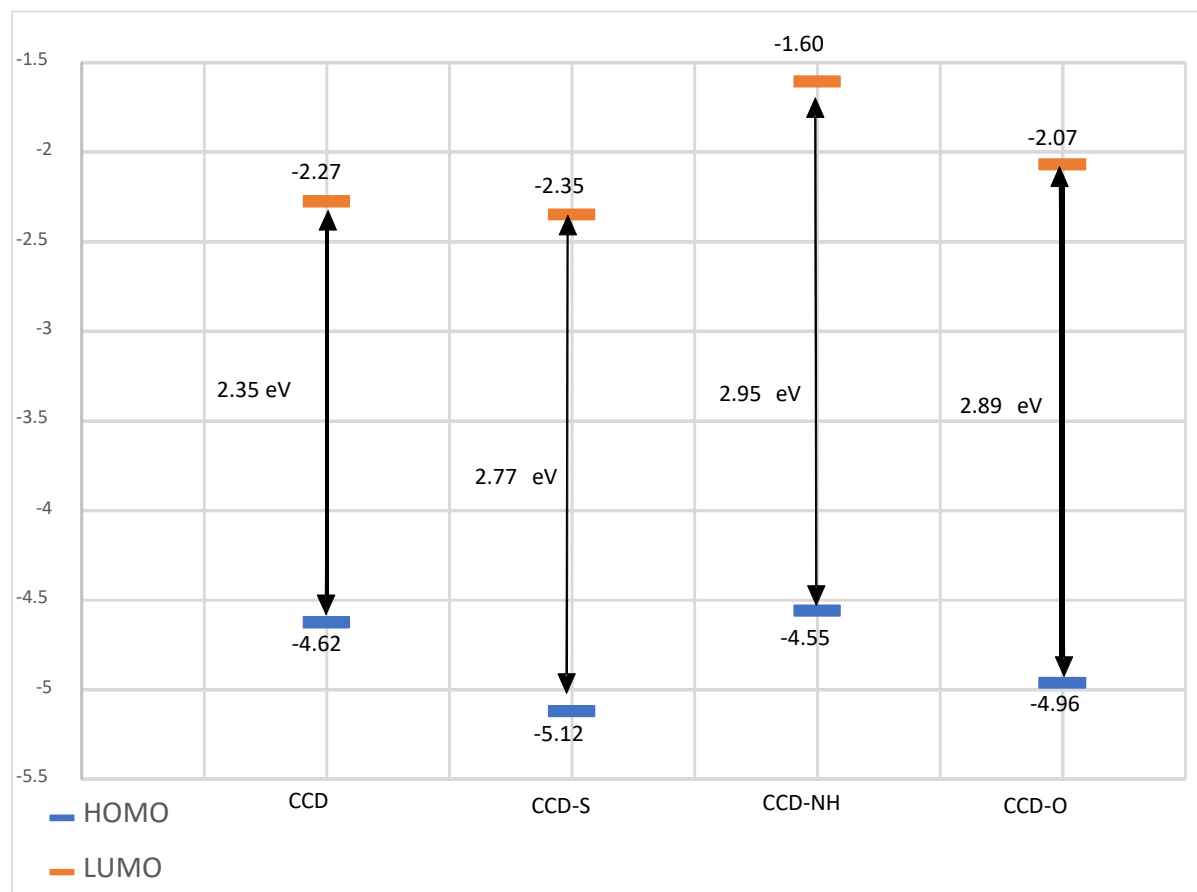
Molecule	HOMO	LUMO
CCD		
CCD-S		
CCD-NH		
CCD-O		

Fig 3: HOMO and LUMO of CCD and its derivatives plotted for iso-surface value of 0.03 au.



**Fig 4:** The HOMO (blue bars) and LUMO(orange bars) energy levels and energy gaps for the studied molecules obtained from B3LYP/6-311G(d,p) level of theory.

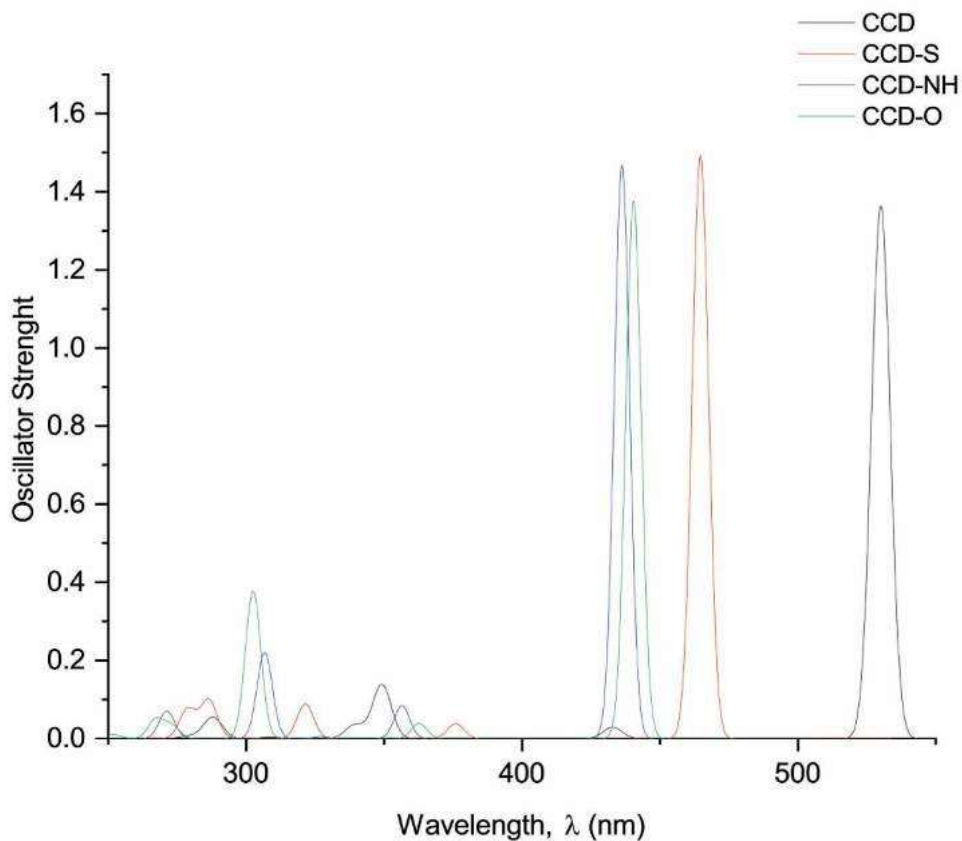
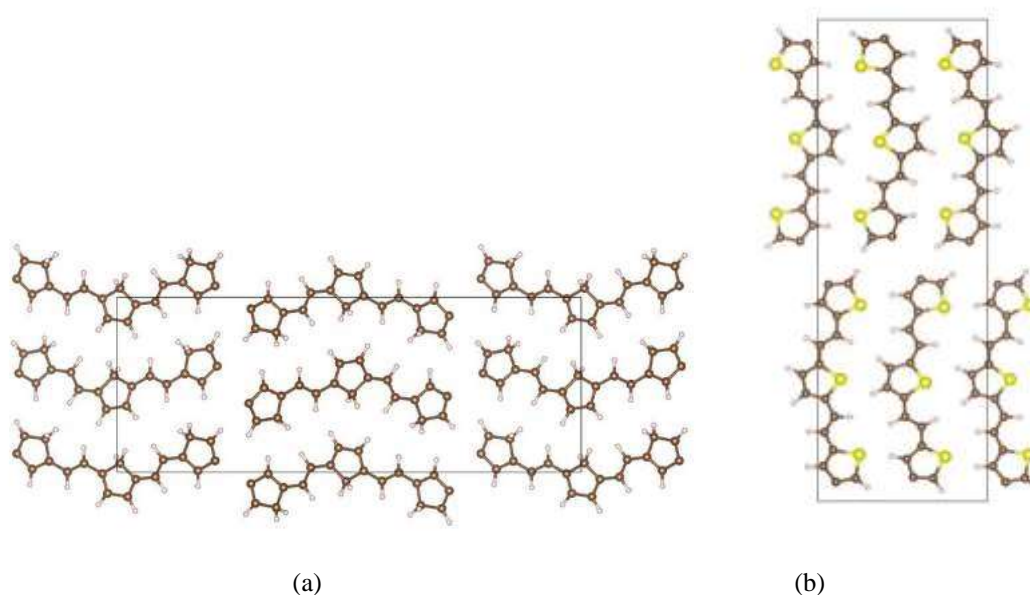
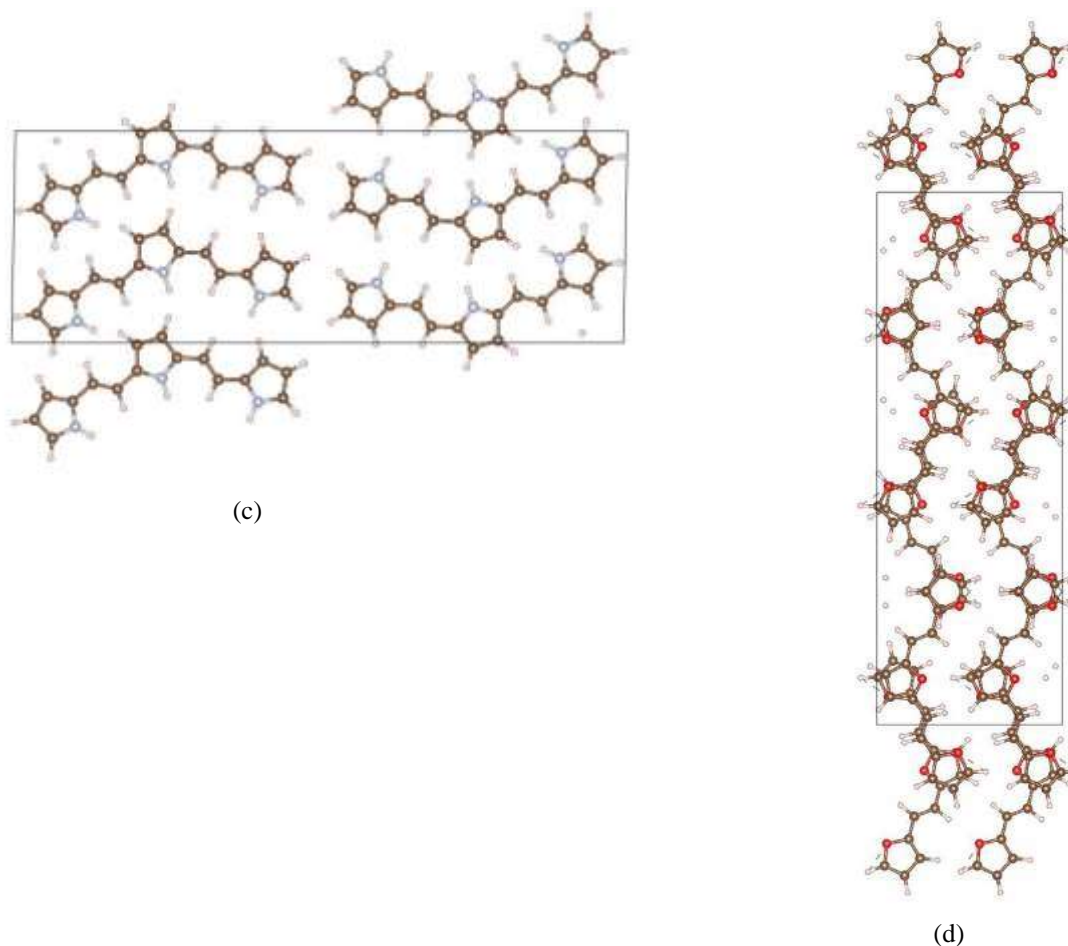


Fig 5: Absorption spectrum of the studied CCD molecules calculated at the B3LYP/6-31+G(d,p) level of theory





**Fig 6:** Predicted crystal structures of (a) CCD, (b) CCD-S, (c) CCD-NH and (d) CCD-O molecules

S.No	Hirshfeld surface	Fingerprint
CCD		



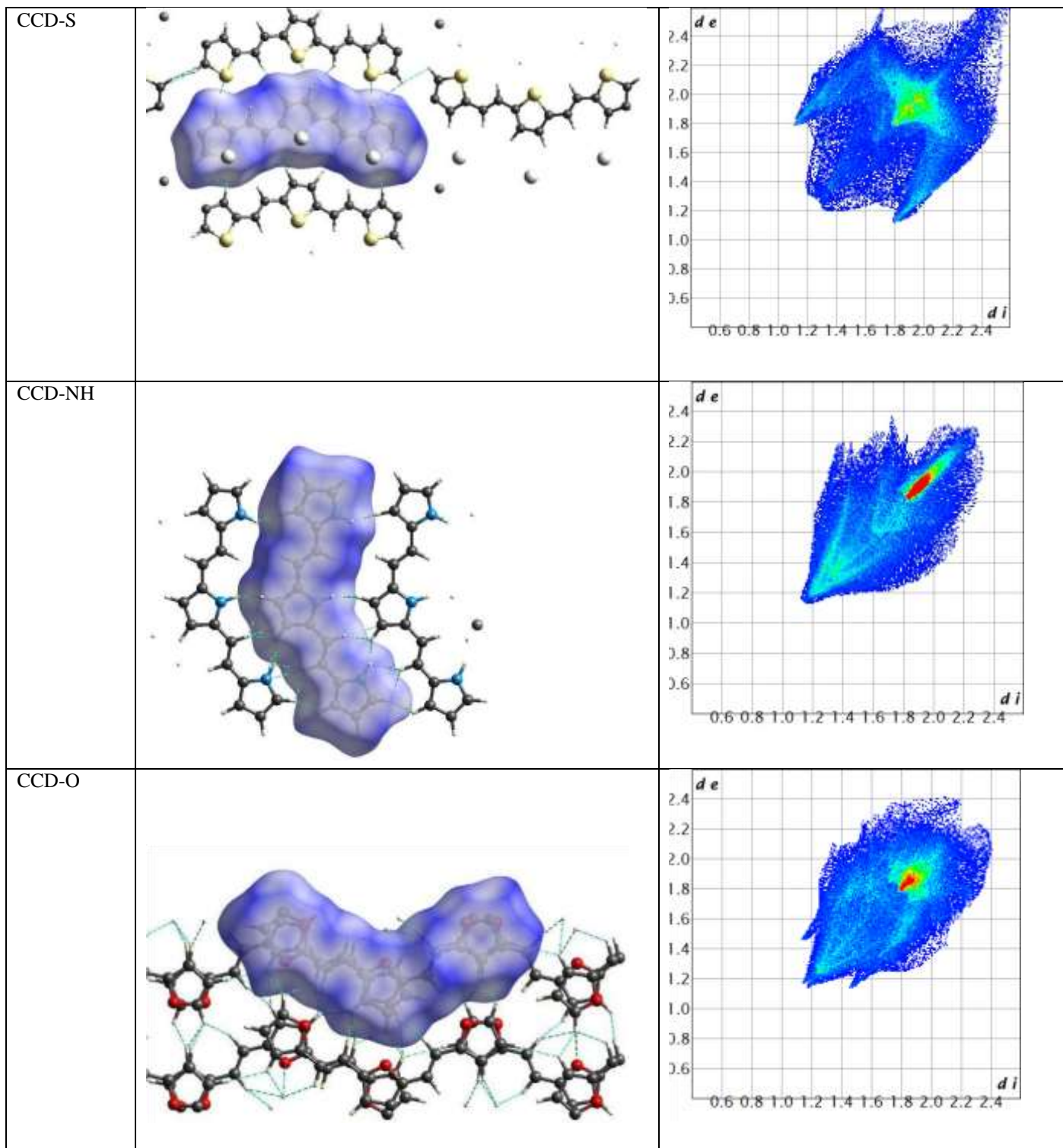


Fig 7: Hirshfeld surface of and 2-dimensional fingerprint plot of intermolecular interactions of CCD systems.

Cite this Article: Mrs. Jothi Balakrishnan, Mr. Stephen A. David, Mr. Palanisamy Subramaniam, Mr. Selvaraju Karuppanan (2023). Charge Transfer and Optical Characteristics of cyclopenta-diene based Oligomers. International Journal of Current Science Research and Review, 6(7), 4822-4835